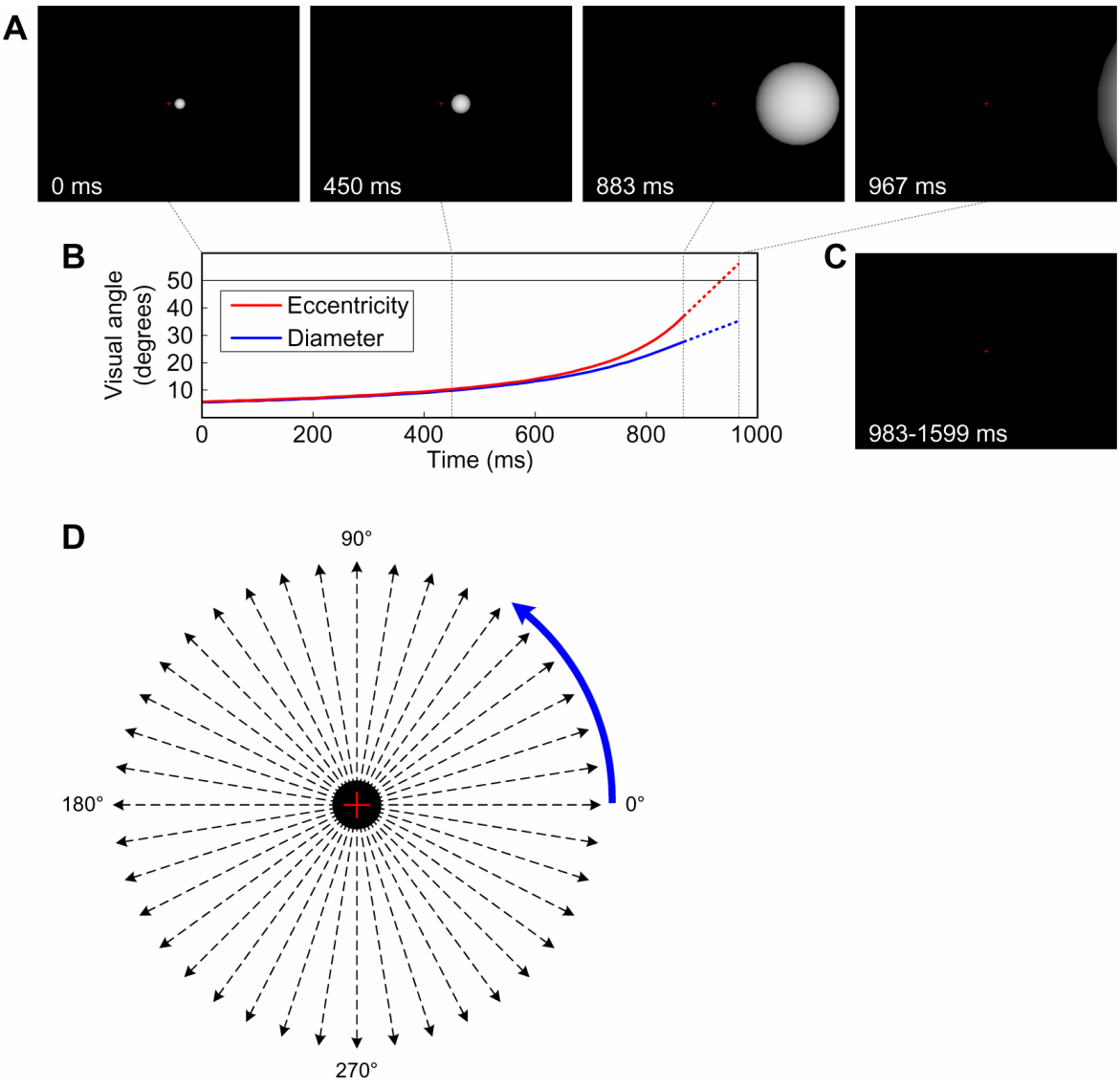

Figure S1. Looming stimuli in Experiment 2. (**A**) Key frames of stimuli in a representative trial where a looming ball approaches along the horizontal meridian (0°). (**B**) Time courses of eccentricity and diameter of the looming ball. (**C**) Fixation cross against a black background after the ball completely disappears at 983ms. (A-C) reproduced from Huang et al. (2012) with permission. (**D**) Schematic trajectories of the looming ball in a 64-s cycle (40 trials/cycle; trials start at 0°, with a 9° increment per trial in the counterclockwise direction).

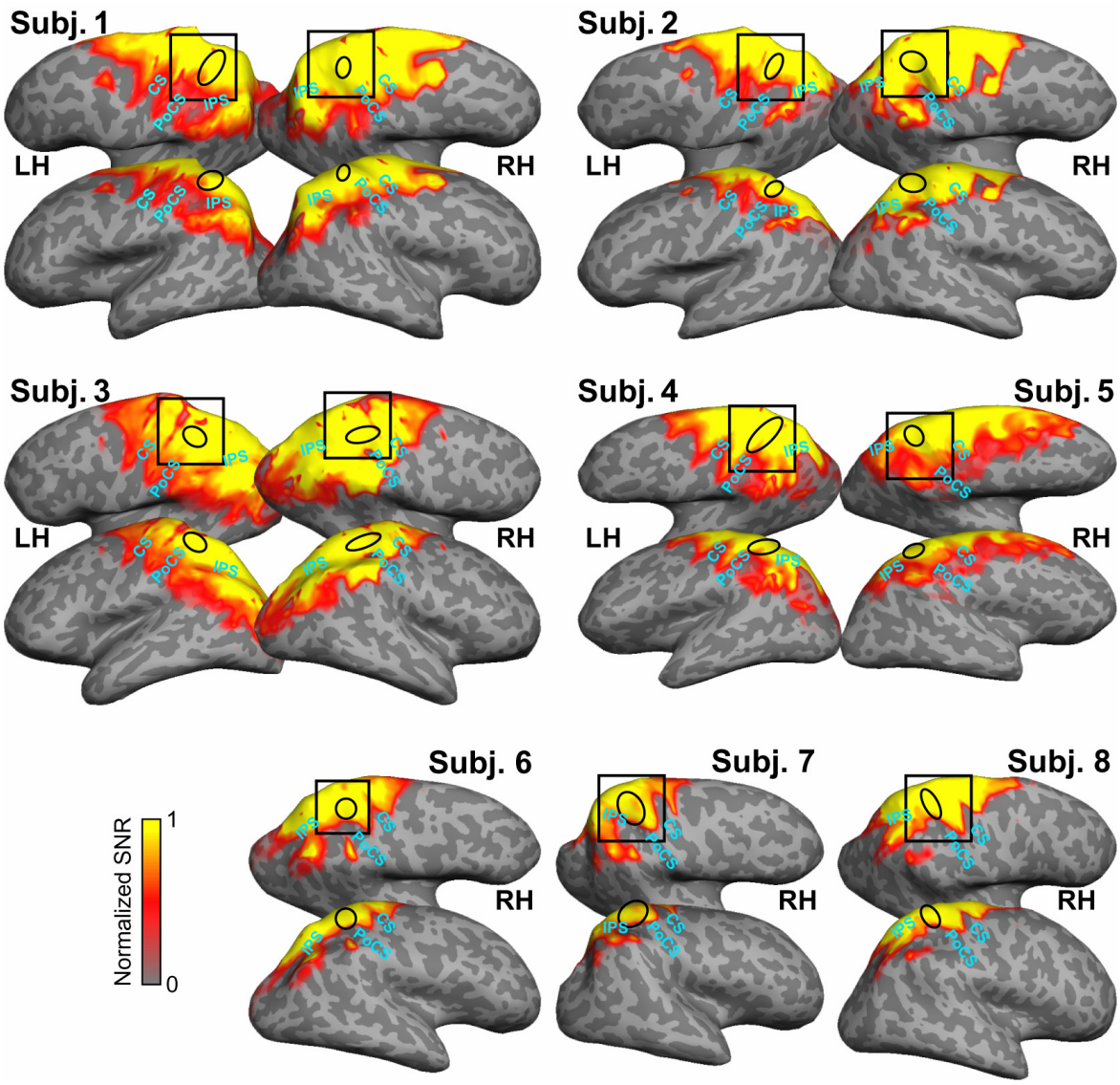

Figure S2. Surface-based maps showing distribution of SNR in functional scans. All maps and sROIs are displayed in the same views as those in Figs. 2 and 3. For each voxel, the normalized SNR is obtained by computing the ratio between the average image intensity (averaged across time course per voxel) and background noise (standard deviation of a non-brain region with 10×10 voxels), and then normalized (between 0 and 1) using a sigmoid function.

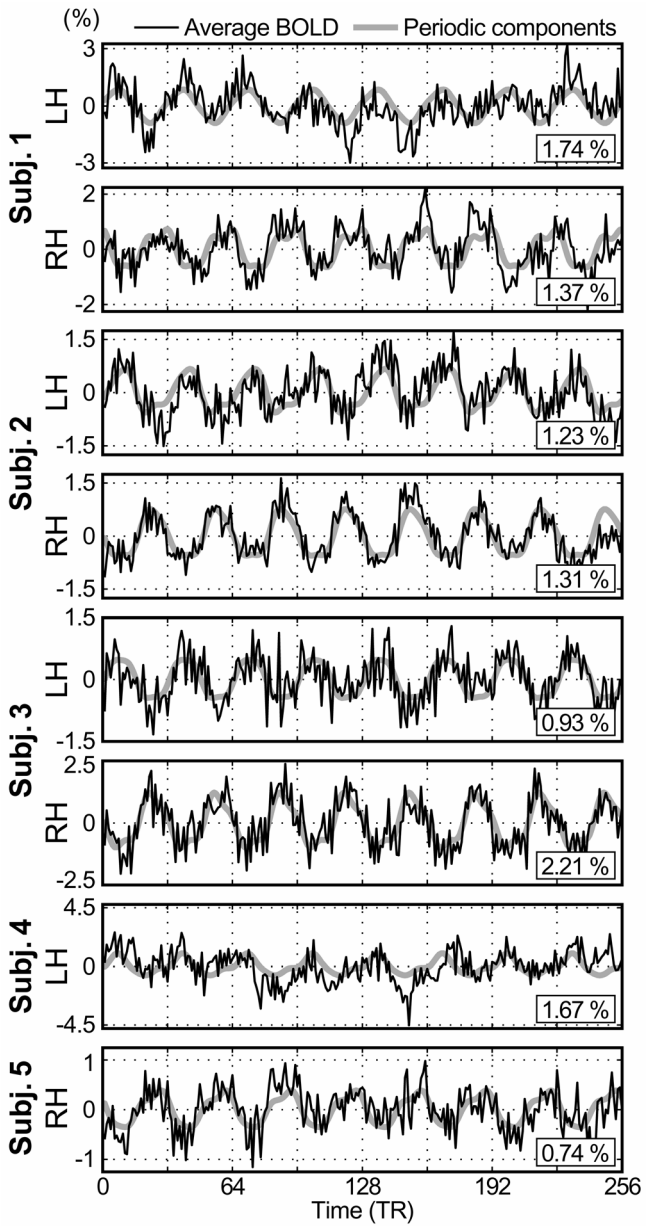

Figure S3. Time courses of BOLD signals averaged across voxels enclosed in the peak activation region within each sROI in Fig. 2. Each thick gray curve represents a periodic waveform reconstructed from the periodic components (harmonics: 8, 16, and 24 cycles per scan) on the Fourier spectrum, with it peak-to-peak signal change indicated in percentage at the lower right corner.

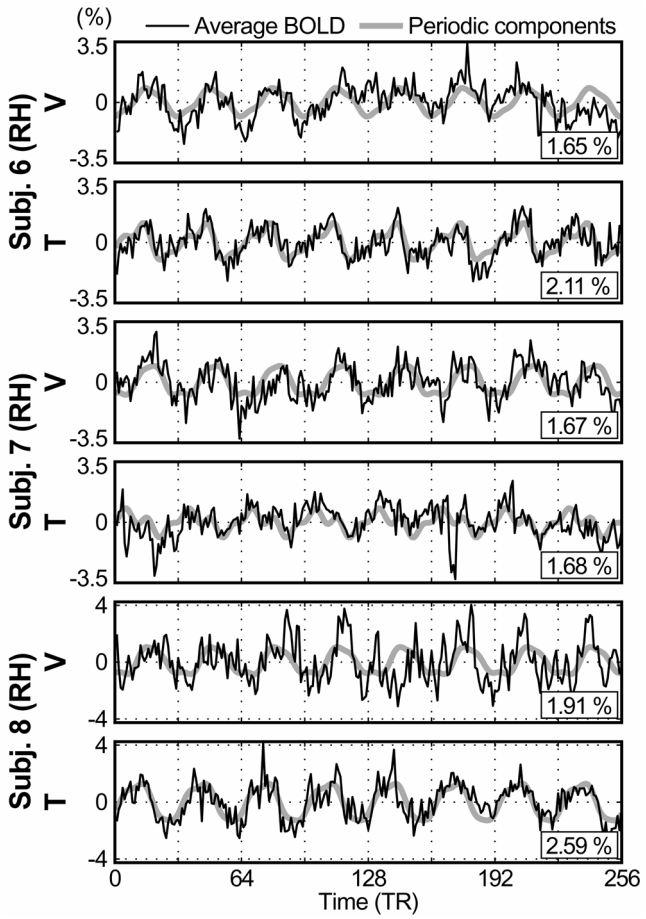

Figure S4. Time courses of BOLD signals averaged across voxels enclosed in the peak activation region within each sROI in Fig. 3. V: visual map (retinotopy); T: tactile map (somatotopy). Other conventions as in Fig. S3.

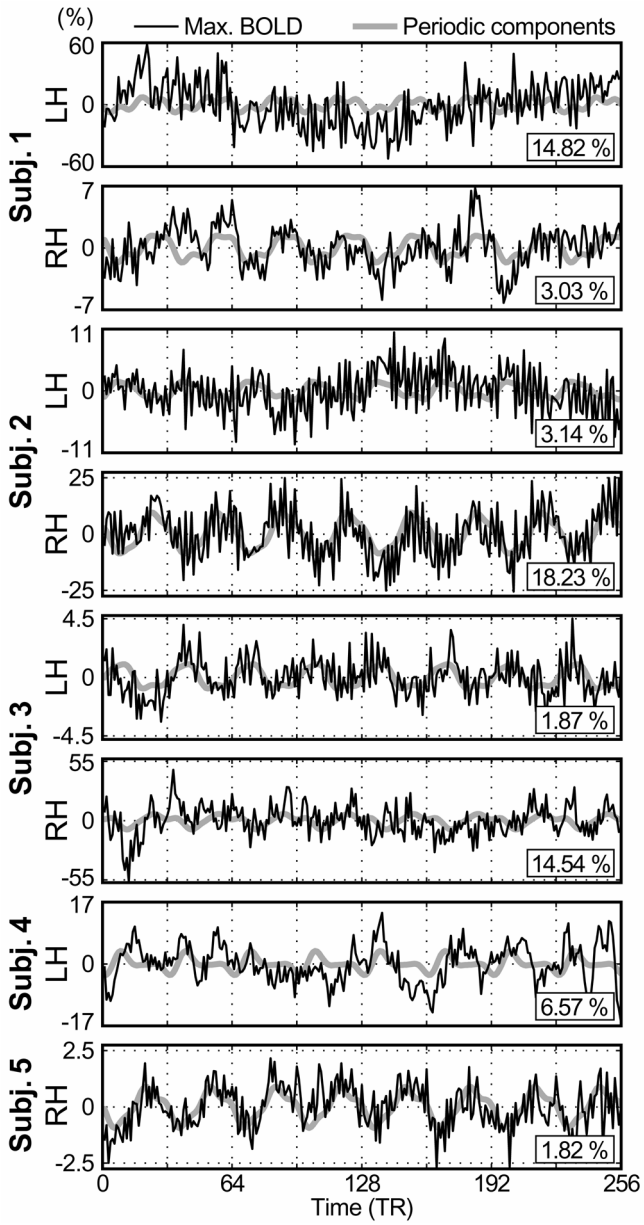

Figure S5. Time course of a single voxel (enclosed in the peak activation region within each sROI in Fig. 2) showing the highest peak-to-peak signal change in the periodic waveform (gray curve) reconstructed from the periodic components (harmonics: 8, 16, and 24 cycles per scan) on the Fourier spectrum. Other conventions as in Fig. S3.

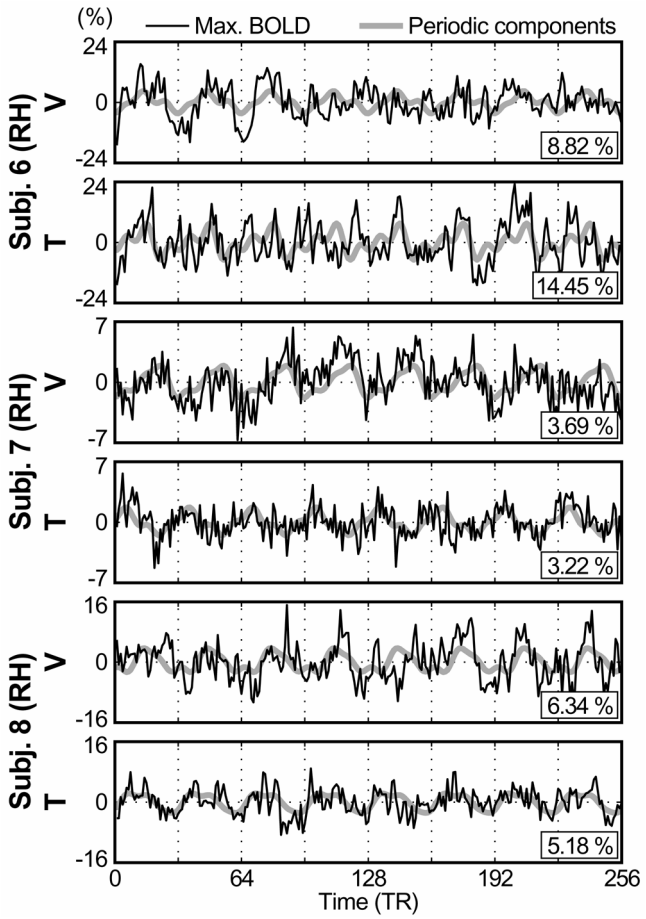

Figure S6. Time course of a single voxel (enclosed in the peak activation region within each sROI in Fig. 3) showing the highest peak-to-peak signal change in the periodic waveform (gray curve) reconstructed from the periodic components (harmonics: 8, 16, and 24 cycles per scan) on the Fourier spectrum. Other conventions as in Fig. S4.

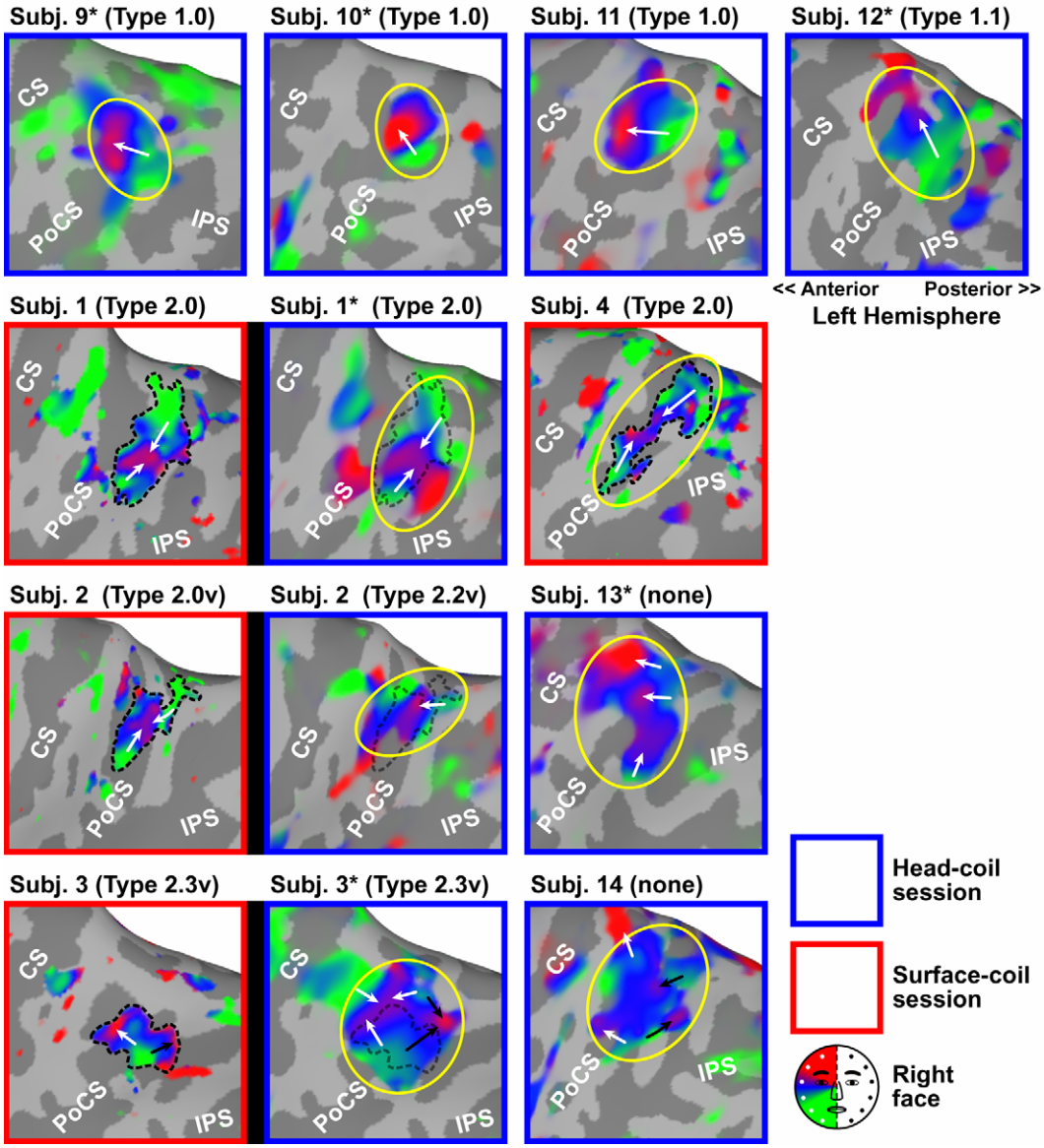

Figure S7. Somatotopic maps of the parietal face area in the left hemispheres of 10 subjects. Each yellow circle outlines the approximate extent of the parietal face area in a subject whose retinotopic map is also present in Fig. S9. Paired maps in head-coil and surface-coil sessions of the same subject are bound together with a black bar. Dashed black contour: sROI of parietal face area in the surface-coil session; White arrow: anterior subdivision; Black arrow: posterior subdivision; CS: central sulcus; PoCS: postcentral sulcus; IPS: intraparietal sulcus; v: variations on a topological type; *: previously published data (Huang and Sereno, 2007; Sereno and Huang, 2006).

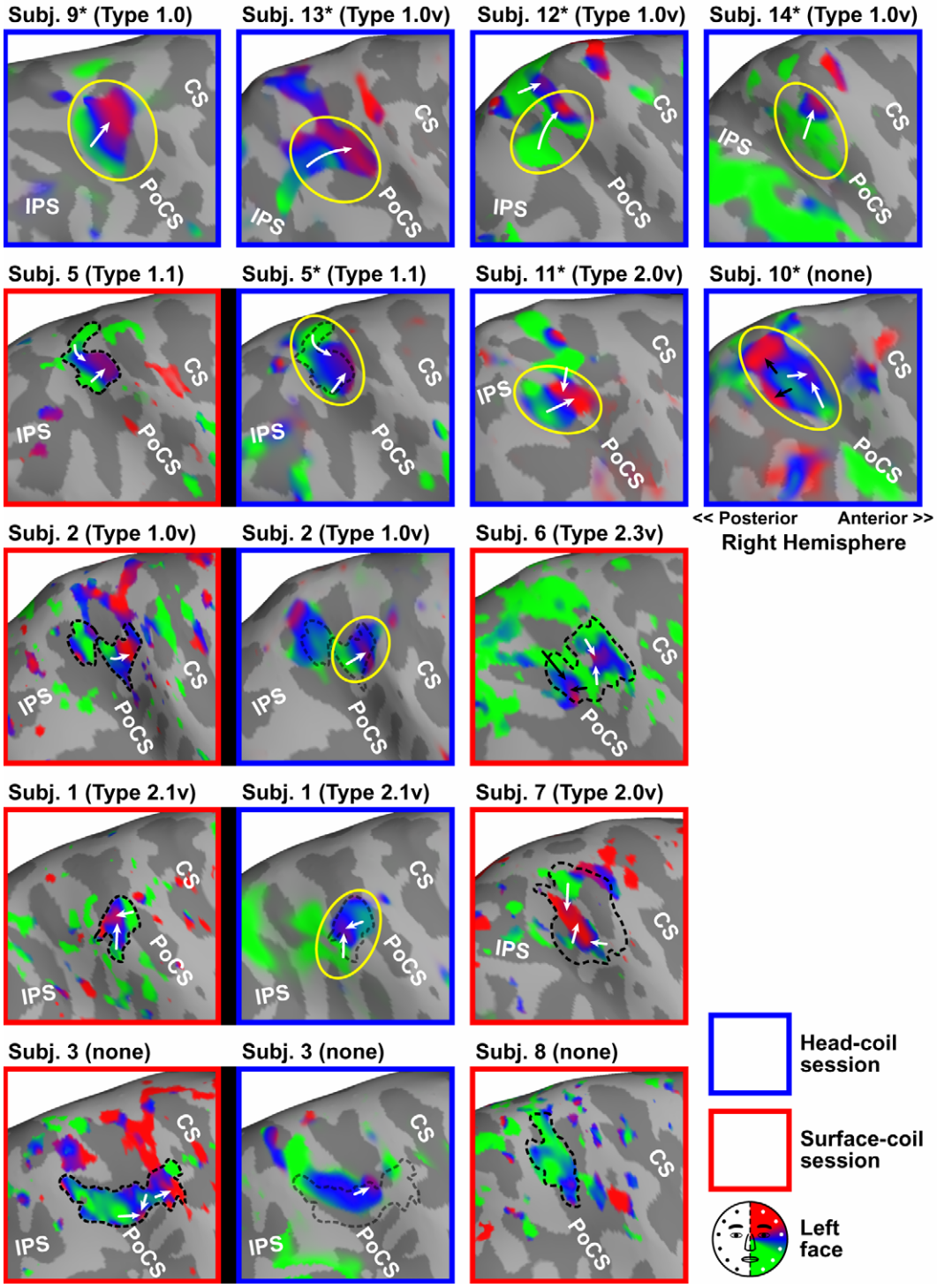

Figure S8. Somatotopic maps of the parietal face area in the right hemispheres of 13 subjects. Each yellow circle outlines the approximate extent of the parietal face area in a subject whose retinotopic map is also present in Fig. S10. *: previously published data (Huang and Sereno, 2007; Sereno and Huang, 2006). Other conventions as in Fig. S7.

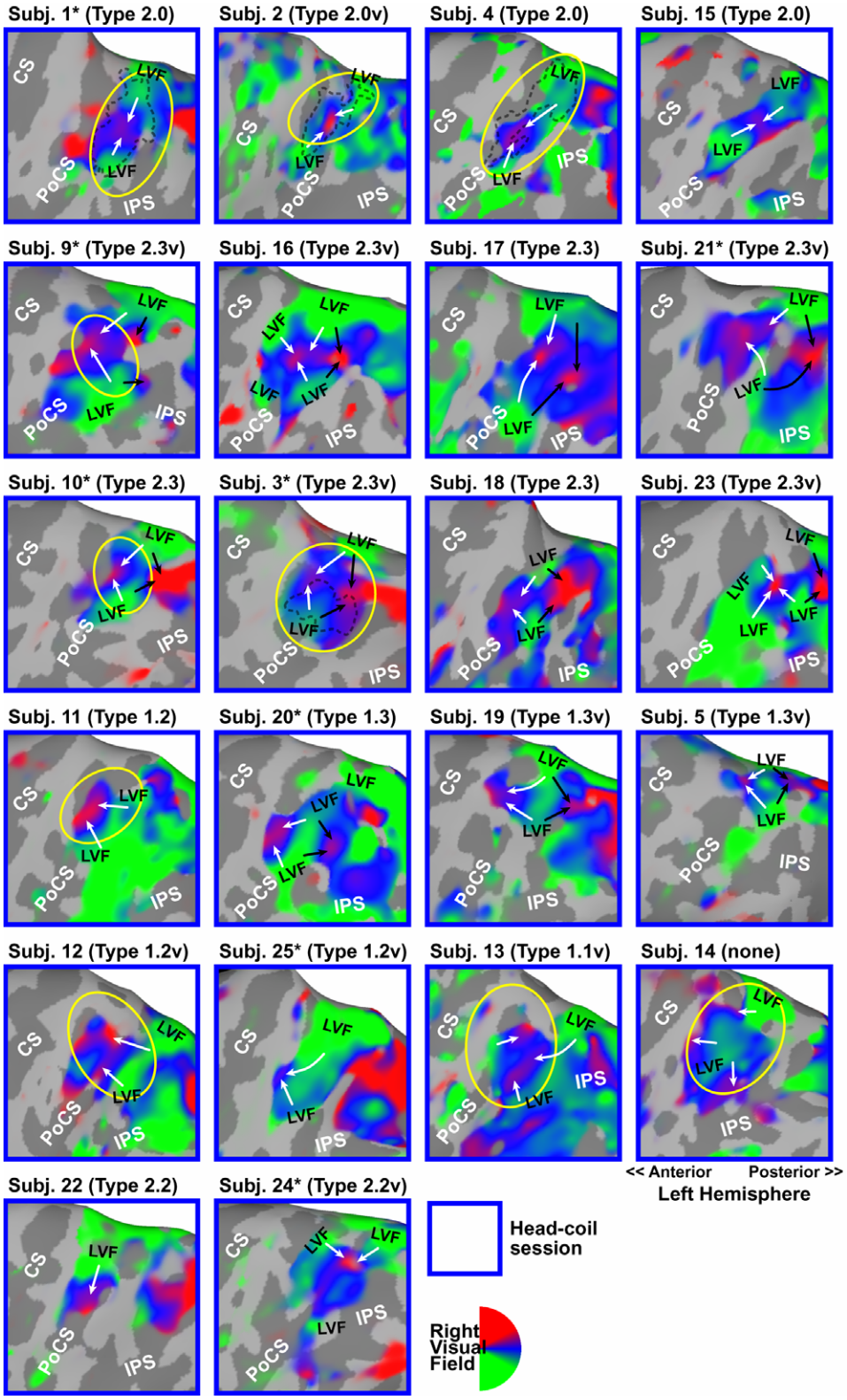

Figure S9. Retinotopic maps of the parietal face area in the left hemispheres of 22 subjects. Yellow circles: see somatotopic maps of corresponding subjects in Fig. S7; LVF: lower visual field; *: previously published data (Huang et al., 2012; Sereno and Huang, 2006). Other conventions as in Fig. S7.

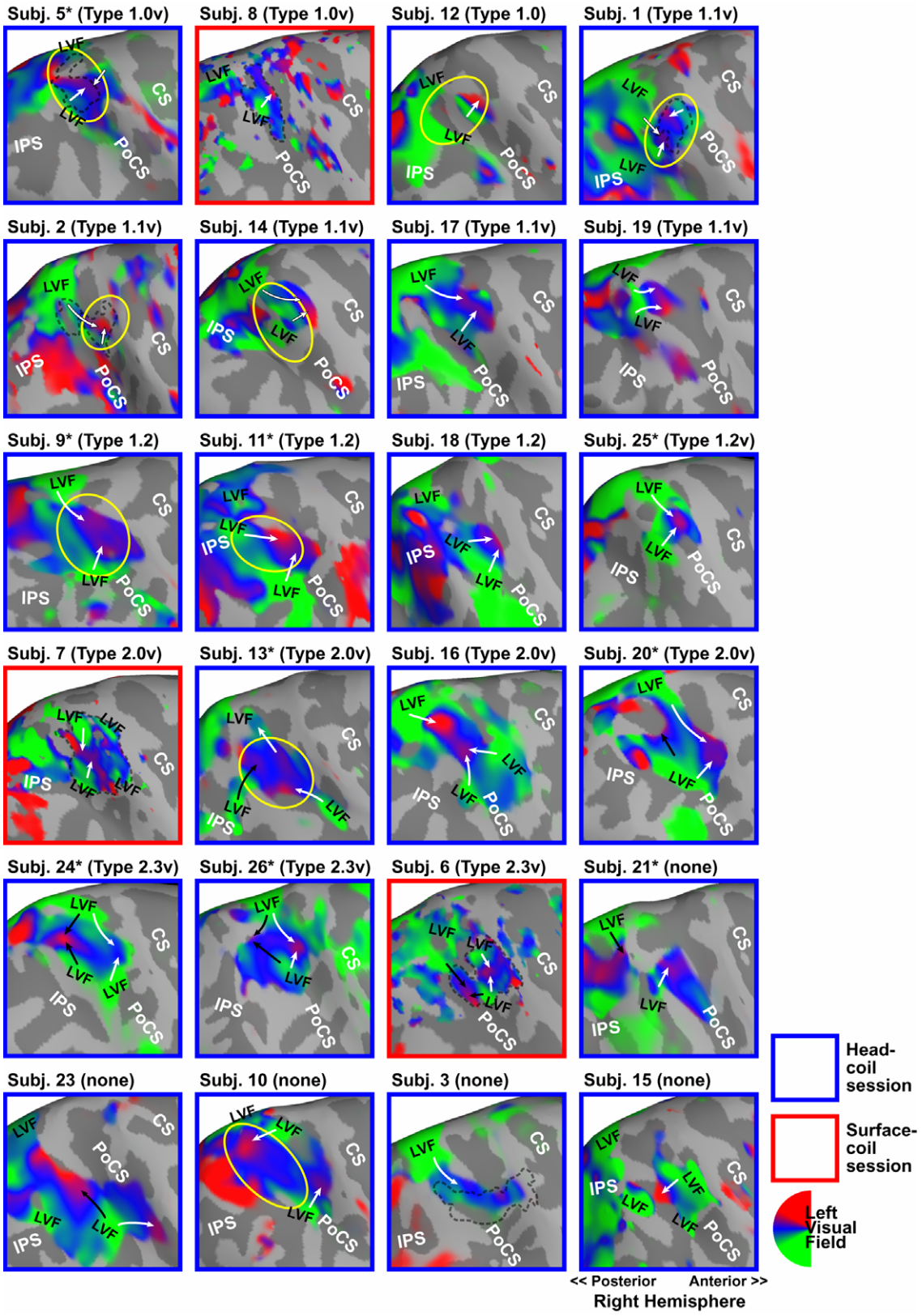

Figure S10. Retinotopic maps of the parietal face area in the right hemispheres of 24 subjects. Yellow circles: see somatotopic maps of corresponding subjects in Fig. S8; LVF: lower visual field; *: previously published data (Huang et al., 2012; Sereno and Huang, 2006). Other conventions as in Fig. S7.